Desorption ionization using through-hole alumina membrane offers higher reproducibility than 2,5-dihydroxybenzoic acid, a widely used matrix in Fourier transform ion cyclotron resonance mass spectrometry imaging analysis

メタデータ	言語: eng
	出版者: John Wiley and Sons
	公開日: 2023-02-09
	キーワード (Ja):
	キーワード (En):
	作成者: Md. Mahmudul, Hasan
	メールアドレス:
	所属:
URL	http://hdl.handle.net/10271/00004265

RESEARCH ARTICLE

Rapid Communications in Mass Spectrometry   WILEY

Desorption ionization using through-hole alumina membrane offers higher reproducibility than 2,5-dihydroxybenzoic acid, a widely used matrix in Fourier transform ion cyclotron resonance mass spectrometry imaging analysis

Md. Mahmudul Hasan[1] | Fumihiro Eto[1] | Md. Al Mamun[1] | Shumpei Sato[1] |
Ariful Islam[1] | A.S.M. Waliullah[1] | Do Huu Chi[1] | Yutaka Takahashi[1] |
Tomoaki Kahyo[1] | Yasuhide Naito[2] | Masahiro Kotani[3] | Takayuki Ohmura[3] |
Mitsutoshi Setou[1,4,5]

[1]Department of Cellular & Molecular Anatomy, Hamamatsu University School of Medicine, 1-20-1 Handayama, Higashi-ku, Hamamatsu, Shizuoka, 431-3192, Japan

[2]Graduate School for the Creation of New Photonics Industries, 1955-1 Kurematsu-cho, Nishi-ku, Hamamatsu, Shizuoka, 431-1202, Japan

[3]Hamamatsu Photonics KK, 314-5 Shimokanzo, Iwata, Shizuoka, 438-0193, Japan

[4]International Mass Imaging Center, Hamamatsu University School of Medicine, 1-20-1 Handayama, Higashi-ku, Hamamatsu, Shizuoka, 431-3192, Japan

[5]Department of Systems Molecular Anatomy, Institute for Medical Photonics Research, Preeminent Medical Photonics Education & Research Center, 1-20-1 Handayama, Higashi-ku, Hamamatsu, Shizuoka, 431-3192, Japan

Correspondence
M. Setou, Department of Cellular and Molecular Anatomy, Hamamatsu University School of Medicine, 1-20-1 Handayama, Higashi-ku, Hamamatsu, Shizuoka 431-3192, Japan.
Email: setou@hama-med.ac.jp

Rationale: DIUTHAME (desorption ionization using through-hole alumina membrane), a recently developed matrix-free ionization-assisting substrate, was examined for reproducibility in terms of mass accuracy and intensity using standard lipid and mouse brain sections. The impregnation property of DIUTHAME significantly improved the reproducibility of mass accuracy and intensity compared with 2,5-dihydroxybenzoic acid (DHB).

Methods: Frozen tissue sections were mounted on indium tin oxide-coated glass slides. DIUTHAME and DHB were applied to individual sections. Subsequently, a solution of a phosphatidylcholine standard, PC(18:2/18:2), was poured onto the DIUTHAME and matrix. Finally, the samples were subjected to laser desorption ionization coupled with Fourier transform ion cyclotron resonance mass spectrometry. The reproducibility was tested by calculating the mean ± standard deviation values of mass errors and intensities of individual ion species.

Results: Analysis of the PC(18:2/18:2) standard showed significantly ($p < 0.01$) lower mass error for DIUTHAME-MS than for MALDI-MS. Endogenous PC(36:4) analysis in mouse brain section also showed significantly ($p < 0.05$) lower mass errors for DIUTHAME-MS. Furthermore, we investigated the mass error of some abundant lipid ions in brain sections and observed similar results. DIUTHAME-MS displayed

lower signal intensity in standard PC analysis. Interestingly, it offered higher signal intensities for all the endogenous lipid ions. Lower fluctuations of both mass accuracies and signal intensities were observed in DIUTHAME-MS.

Conclusions: Our results demonstrated that DIUTHAME-MS offers higher reproducibility for mass accuracies and intensities than MALDI-MS in both standard lipid and mouse brain tissue analyses. It can potentially be used instead of conventional MALDI-MS and mass spectrometry imaging analyses to achieve highly reproducible data for mass accuracy and intensity.

1 | INTRODUCTION

Mass spectrometry imaging (MSI) is a label-free molecular imaging technique that allows the simultaneous mapping of hundreds of molecules in tissues or cells. Various ionization techniques such as matrix-assisted laser desorption ionization (MALDI),[1] desorption electrospray ionization,[2] and secondary ion[3] have been used in MSI for the visualization of proteins,[4] fatty acids,[5] phospholipids,[6,7] nucleotide,[8] neurotransmitters,[9] small metabolites, and exogenous compounds[10,11] in a wide range of biological samples. MALDI-MSI is currently the most widely used MSI technique where thin tissue sections are generally thaw-mounted on an indium tin oxide (ITO)-coated glass slide and subsequently coated with a matrix solution, resulting in the formation of co-crystals between the matrix molecules and the analytes. The sample surface is then irradiated by laser energy that causes the rapid heating of the matrix molecules. Consequently, the heated molecules, as well as the analytes, undergo desorption and ionization. Ionization of the analytes is thought to occur through charge transfer between the excited matrix molecules and the neutral analytes.[12,13]

MALDI-MSI has been shown to have the capability of detecting molecules with higher sensitivity in a wide mass range than the other MSI techniques. However, the quality and the reproducibility of MALDI data are directly affected by the sample preparation method.[14] The results often differ from person to person, even from experiment to experiment, due to the difficulty in maintaining identical conditions for matrix application.[15,16] Homogenous spraying has been achieved by the emergence of automatic matrix sprayers, such as the TM-Sprayer™ (HTX Technologies, Carrboro, NC, USA) or the iMLayer™ (Shimadzu Co. Ltd, Kyoto, Japan), although these are costly and the procedure is time-consuming.[13] To combat matrix crystal heterogeneity, ionic liquid matrices (ILMs) have been reported to offer higher signal intensity, enhanced spot homogeneity, increased signal reproducibility, and similar or better detection limits compared with the widely used crystalline matrix 2,5-dihydroxybenzoic acid (DHB). Unfortunately, the use of ILMs provides a stronger tendency for alkali metal–ion adduct generation.[17] In addition, the optimization of ILMs is a trial-and-error process, and the base-to-acid ratio can alter the performance of these materials.[18] Thus, sample preparation is still a bottleneck in achieving reproducible data in MALDI-MS and MSI analyses.

High mass accuracy acts as a powerful "filter" that significantly limits the number of possible molecular formulae.[19,20] Therefore, high reproducibility of accurate mass measurements is essential for characterizing small molecules.[21,22] Fourier transform MS or Fourier transform ion cyclotron resonance (FTICR) MS facilitates the highest mass accuracy and resolving power among all the most frequently used MS techniques over a broad m/z range.[23–25] Even for a small number of ions, it outperforms many other frequently applied MS methods.[26] Our group has previously exploited this advantage of FTICR to explore active chemical components in a traditional beverage.[27] However, the space charge effects caused by a high number of ions derived from the DHB matrix have been reported to reduce the reproducibility of accurate mass measurements.[28]

Surface-assisted laser desorption ionization (SALDI) is an alternative technique, which uses the optophysical properties of solid compounds rather than the spectral properties of organic matrix compounds. It could be a useful technique for detecting low-mass molecules from the sample without matrix-derived peaks.[29] Previously, matrix-free laser desorption ionization methods have been described that are based on nanostructure surfaces such as nanomaterial-assisted laser desorption ionization,[30–32] desorption ionization on silicon,[33,34] silicon nanowires,[35] clathrate nanostructures,[36] silicon nanoparticles,[37] and silicon nanopost arrays[38–44] for the analysis of biological samples and exogenous molecules. In such laser desorption ionization methods, a sufficient amount of sample must be deposited appropriately to allow the penetration of the laser into the sample layer. Otherwise, the thick layer of sample causes laser beam decay.[36] In addition, the preparations of those inorganic materials can be complex and costly.[29] The regularity and the diameters of the nanoposts are highly critical for achieving optimized results.[45]

Recently, our group has developed novel ionization-assisting membrane chips based on SALDI procedures that use a porous alumina membrane called desorption ionization using through-hole alumina membrane (DIUTHAME). The capillary action of DIUTHAME has a very large aspect ratio across the through-hole alumina membrane that enables many loading protocols, including sample impregnation from the opposite side to the laser exposure surface. It is assumed that the size and shape of the through-holes lead to the conversion and transfer of photon

energies. Previously, our group reported that the ionic yield depends to some degree on the inner diameter of the through-hole alumina membrane.[46]

Successful feasibility studies in which a DIUTHAME chip was applied for the MS study of liquid samples[46] and MSI analysis of brain tissue sections of mice[47] were previously reported. In contrast to MALDI, DIUTHAME is a matrix-free ionization-assisting method; thus, interference induced by matrix-derived ion peaks in the lower mass range, generally found in MALDI-MS, is not observed in DIUTHAME-MS analyses.[46–48] In addition, DIUTHAME significantly reduces the sample preparation time and does not require a qualified technician or specialized instrument for matrix application.[46,47]

In the study presented here, we used a DIUTHAME chip in the preparation of standard lipid and mouse brain tissue samples followed by FTICR MS analysis to investigate the reproducibility of mass accuracies and signal intensities of the measured ions. The results were compared with those obtained using MALDI-MS, where DHB was used as a matrix.

2 | EXPERIMENTAL

2.1 | Materials

Methanol (MeOH) and ultrapure water, DHB, and phosphatidylcholine PC(18:2/18:2) were purchased from Wako Pure Chemical Industries (Osaka, Japan), Bruker Daltonics (Fremont, CA, USA), and Avanti Polar Lipids (Alabaster, AL, USA), respectively. DIUTHAME chips (A13331-18-1) were provided by Hamamatsu Photonics K.K. (Shimokanzo, Shizuoka, Japan). These chips (18 mm in diameter) were the same as the commercially available products of Hamamatsu Photonics. The shape of the through-holes, the developmental procedures, and characteristics have been previously described in detail.[46] All materials used in this study were of the highest purity.

2.2 | Sample preparation for MS analysis

All experimental protocols and procedures for animals were conducted in accordance with the guidelines set by the Ethics Committee of Hamamatsu University School of Medicine (Hamamatsu, Japan) and conducted following the approved guidelines.

Two C57BL/6J male mice (age: 90 days) purchased from SLC Inc. (Hamamatsu, Japan) were used in this study. The mouse brains were excised after euthanasia by cervical dislocation and subsequently frozen in powdered dry ice and stored at −80°C in a refrigerator until analysis. The frozen tissues were cryosectioned (coronal section; 10 μm for MALDI-MS and 30 μm for DIUTHAME-MS) at −20°C using a CM1950 cryostat (Leica Biosystems, Buffalo Grove, IL, USA). The DIUTHAME chip was then applied on the tissue section of the mouse brain, as described previously.[47] Briefly, inside the cryostat chamber,

the tissue section of the mouse brain (30 μm thick) was mounted on a precooled conductive ITO-coated glass slide (100 Ω; Matsunami, Japan), and a precooled DIUTHAME chip was placed very gently onto the tissue section (Figure 1). A finger was pressed (2–3 min) straight down onto the tissue slice on the ITO-coated glass slide such that the molecules in the tissue sample could thaw and be raised off the upper surface of the DIUTHAME by capillary action and then allowed to dry for 5–10 min. An amount of 1 μL of a solution of a PC(18:2/18:2) standard (diluted 200 times in 100% MeOH from the stock (2.5 mg/mL in 100% MeOH)) was added via a dropper onto the DIUTHAME chip where the tissue section was absent. Another serial mouse brain tissue section (10 μm thick) was mounted on an individual ITO-coated glass slide for matrix application. DHB solution (40 mg/mL in 50% MeOH) was sprayed automatically using a TM-Sprayer™ (HTX Technologies). The parameters for the TM-Sprayer™ were set as follows: spray gas pressure, 10 psi; nozzle temperature, 80°C; the number of spray cycles, 24; speed of nozzle movement, 1250 mm/min; flow rate, 0.05 mL/min. After matrix spraying, 1 μL of a solution of the PC(18:2/18:2) standard was added via a dropper onto the matrix-coated ITO-coated glass slide where the tissue section was absent. Samples were then sent to the FTICR mass spectrometer for measurement.

2.3 | Mass spectrometer calibration

Before analysis, the calibration of the FTICR mass spectrometer was carried out with sodium formate (1 mg/mL in 50% MeOH) cluster ions. The sodium formate solution was externally injected directly into the ESI source, and the data were acquired in the mass range m/z 500–1200. The standard deviations (SDs) were calculated based on five measurements under identical experimental conditions where the resultant mass errors were less than 1 ppm (Figure S1 and Table S1, supporting information).

The applied function of the calibration used for converting the ion cyclotron frequencies to m/z values is represented as Equation 1, where A and B are the calibration constants and f is the calculated frequency:

$$\frac{m}{z} = \frac{A}{f} + \frac{B}{f^2}$$

(1)

This calibration equation was initially derived by Ledford et al.[49] According to this derivation, the second term, B/f^2, denotes the field of direct current trapping and the effect of space charge.

2.4 | Data acquisition and analysis

Mass spectra were acquired in positive ion mode using a SolariX XR FTICR mass spectrometer (Bruker Daltonik, Bremen, Germany), which was equipped with a superconducting magnet (7.0 T) and a Bruker Smartbeam II™ laser (355 nm). Bruker Daltonik ftmsControl software
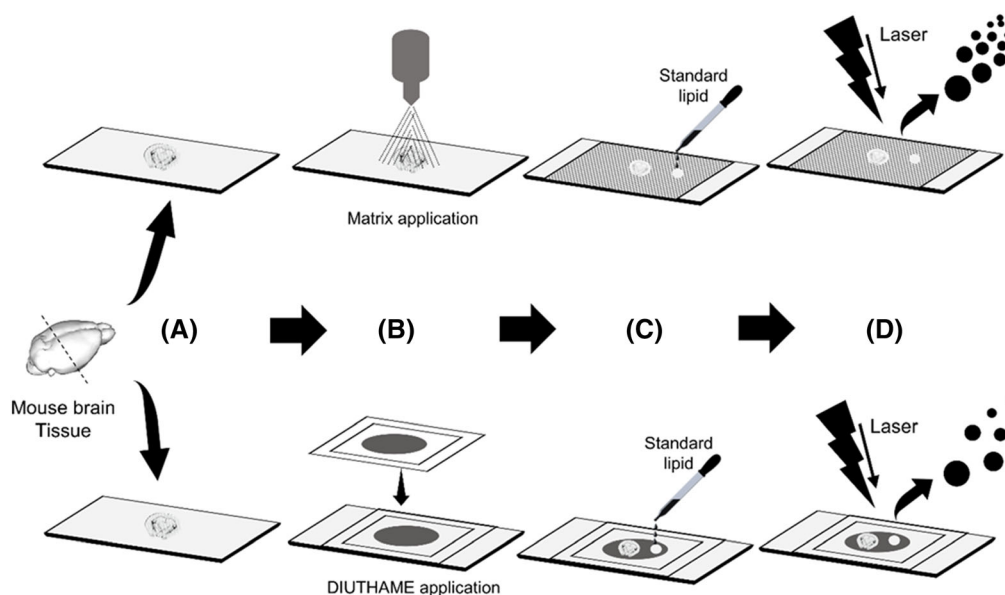
FIGURE 1 Sample preparation workflow for standard lipid and frozen tissue sections in MALDI-MS and DIUTHAME-MS. (A) Frozen tissue sections obtained by cryosectioning were mounted on ITO-coated glass slides. (B) DHB was sprayed using an automated TM-sprayer™ (upper panel). The DIUTHAME chip was placed gently on an individual tissue section before being thawed inside the cryostat (lower panel). The DIUTHAME chip has adhesive areas on the bottom side and can be attached to the ITO-coated slide. Tissue analytes were extracted and transferred upward by the capillary action of the through-holes membrane. (C) After drying, standard lipid was poured onto the matrix (upper panel) and DIUTHAME chip (lower panel) where the tissue sections were absent. (D) Samples were then measured by laser desorption ionization coupled with FTICR MS

was used for data acquisition in the mass range m/z 700–900. The optimized transient length and estimated resolving power in standard lipid analysis were 4 M (13.42 s duration) and 1 800 000 (at m/z 400), respectively. On the other hand, a transient length of 1 M (3.35 s duration) and an estimated resolving power of 450 000 (at m/z 400) were used for tissue section analysis. The time of flight and the Q1 mass were set at 1.00 ms and m/z 700, respectively. The laser focus was set to "small" (dimension was ca 25 μm). The number of laser shots per pixel was 500 at a repetition rate of 1000 Hz. The ion transfer optics settings were optimized to provide the sensitivity and resolving power for MS analysis and are provided in Table S2 (supporting information). The laser power for DIUTHAME-MS was optimized as 25% (for the lipid standard) and 14.5% (for tissue sections). On the other hand, the optimized laser power for MALDI-MS was 15% and 14% for the lipid standard and tissue sections, respectively. The average mass spectra for individual experiments were acquired by irradiating at five different positions on the sample surface in random walk mode. Data analysis was performed using Data Analysis v4.4 (Bruker Daltonik) and FlexImaging (version 4.1, Bruker Daltonik) software. The matrix-related peaks were confirmed by measuring DHB without samples. The extracted ions were processed using a window of 0.02 m/z units. Assignments of compounds other than PC(18:2/18:2) were performed by precisely matching the mass spectra with previously reported data[50–54] and free online databases, including Human Metabolome Database (https://hmdb.ca/), LIPID MAPS® Lipidomics Gateway (https://www.lipidmaps.org/) and Metlin (https://metlin.scripps.edu), considering the mass error to be <5 ppm.

We calculated the mass accuracies (expressed in ppm) by subtracting the theoretical m/z values from the observed m/z values obtained from three experiments under identical conditions. The mean and SD of those mass accuracy values were then calculated. The absolute intensity values of each ion observed in three individual experiments were calculated as mean ± SD.

Microsoft Excel (version 2019) and SPSS Statistics v22.0 (IBM, Armonk, NY, USA) software were used for the statistical analyses. All data were presented as mean ± SD and considered statistically significant at $p < 0.05$.

3 | RESULTS

3.1 | Analysis of PC(18:2/18:2) standard

We performed DIUTHAME-MS and MALDI-MS using the PC(18:2/18:2) standard and acquired mass spectra in the positive ion mode. In both methods, PC(18:2/18:2) was detected as a protonated adduct $[M + H]^+$ at m/z 782.5694. As expected, we observed fewer peaks in DIUTHAME-MS than in MALDI-MS (Figure S2, supporting information). The mass errors for DIUTHAME-MS and MALDI-MS were −0.021 ppm (Figure 2A) and −0.894 ppm (Figure 2B), respectively. Statistically, the mass accuracy for DIUTHAME-MS was significantly ($p < 0.01$) higher with a smaller SD than that for MALDI-MS (Figure 2C). These results indicated that DIUTHAME-MS provides higher
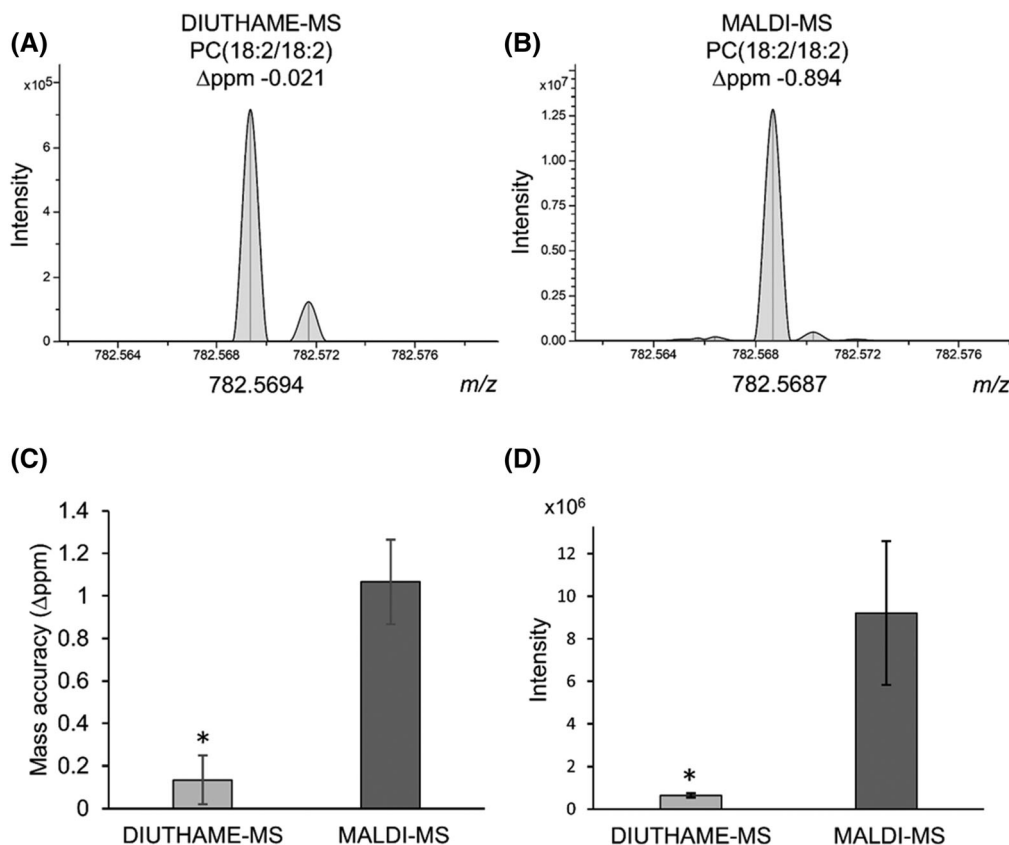
FIGURE 2 Standard lipid analyses show a higher mass accuracy and lower intensity for DIUTHAME-MS than for MALDI-MS. Representative peaks of standard PC(18:2/18:2) at m/z 782.5694 in (A) DIUTHAME-MS and (B) MALDI-MS with their mass accuracies (expressed in ppm). (C) Significant differences (*$p < 0.01$) in mass accuracies between DIUTHAME-MS (m/z and mass accuracy: 782.5694 and 0.135 ± 0.115) and MALDI-MS (m/z and mass accuracy: 782.5687 and 1.066 ± 0.198). (D) Significant differences (*$p < 0.01$) in average intensities between DIUTHAME-MS (m/z and intensity: 782.5694 and 645 239.333 ± 106 699.794) and MALDI-MS (m/z and intensity: 782.5687 and 9 209 235.667 ± 3 379 358.946). DIUTHAME-MS showed a lower SD in mass accuracy and intensity measurements than MALDI-MS. The values are presented as mean ± SD of three measurements. Here, *$p < 0.01$ (two-tailed t-test)

reproducibility in mass accuracy measurements using a lipid standard than MALDI-MS. However, the average intensities in DIUTHAME-MS were significantly ($p < 0.01$) lower than in MALDI-MS (Figure 2D).

3.2 | Endogenous PC(36:4) analysis in brain tissue

To verify the reliability of the highly reproducible data for DIUTHAME-MS, we examined the mass accuracy and intensity of an endogenous PC(36:4), which was used against the PC(18:2/18:2) standard in mouse brain tissue sections at m/z 782.569. The mass errors of DIUTHAME-MS and MALDI-MS were −3.961 ppm (Figure 3A) and −4.472 ppm (Figure 3B), respectively. The mass accuracy and intensity values for endogenous PC(36:4) were significantly ($p < 0.05$) higher with a smaller SD for DIUTHAME-MS than for MALDI-MS (Figures 3C and 3D). These results showed that DIUTHAME-MS also provides higher reproducibility in mass accuracy and intensity measurements in mouse brain tissue sections than MALDI-MS.

3.3 | Analyses of some abundant lipids in brain tissue

For further confirmation of the high reproducibility, we selected several abundant peaks associated with lipid molecules, including m/z 760.585, 772.525, 782.569, 788.616, 798.541, 720.525, and 726.573, in the mouse brain tissue sections, and calculated the mass errors obtained using both DIUTHAME-MS and MALDI-MS (Figures 4A and 4B, respectively). The mass accuracy values for all the selected ions were significantly ($p < 0.05$) higher with a smaller SD for DIUTHAME-MS than for MALDI-MS (Figure 4C). Of the seven ions, two (m/z 782.569 and 798.541) showed significantly ($p < 0.05$) higher intensities in DIUTHAME-MS than in MALDI-MS (Figure 4D). Here, DIUTHAME-MS also showed a smaller SD in intensity measurements for all selected ions than MALDI-MS. These results indicated that DIUTHAME-MS offers higher reproducibility in mass accuracy and intensity measurements than the DHB matrix for mouse brain tissue lipids.

Next, we showed the distribution of mass accuracy and intensity values for the selected lipid ions in the mouse brain section using dot plots. Interestingly, DIUTHAME-MS showed smaller fluctuations in
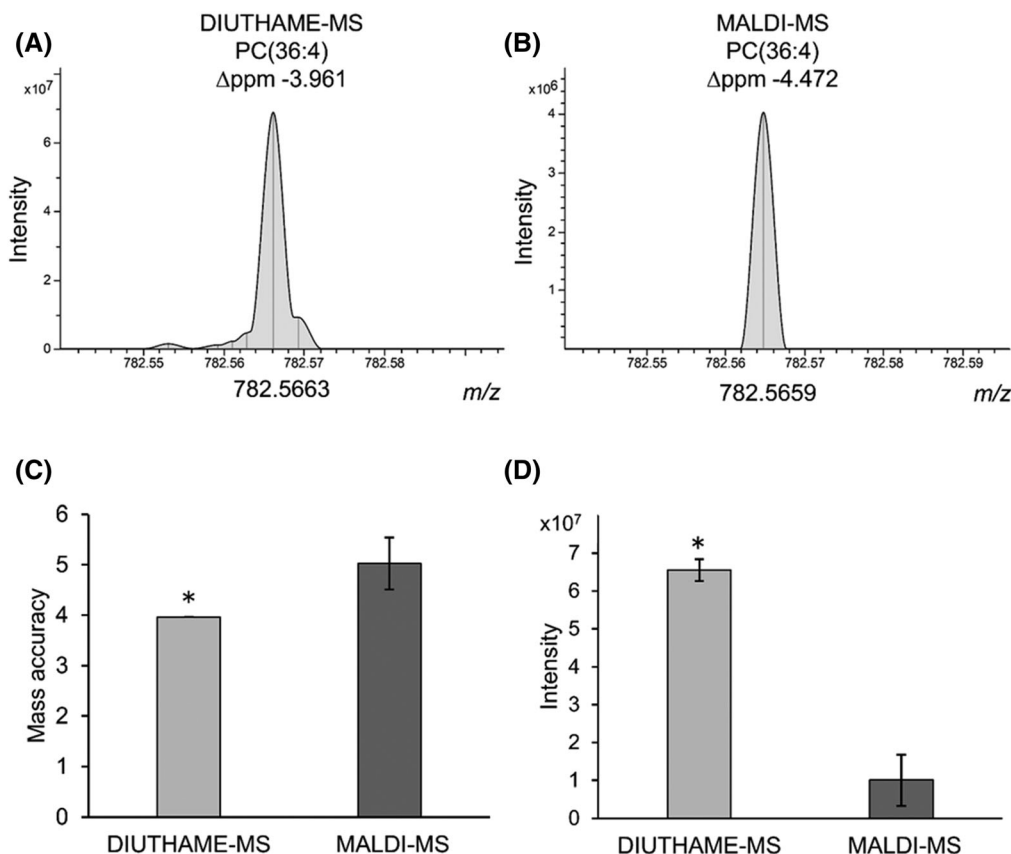
FIGURE 3 Analyses of endogenous PC(36:4) in mouse brain section show a higher mass accuracy and intensity with smaller SD in DIUTHAME-MS than in MALDI-MS. Representative peaks of endogenous PC(36:4) at m/z 782.5694 in (A) DIUTHAME-MS and (B) MALDI-MS with their mass accuracies (expressed as ppm). (C) Significant differences (*$p < 0.05$) in mass accuracies between DIUTHAME-MS (m/z and mass accuracy: 782.5663 and 3.961 ± 0.001) and MALDI-MS (m/z and mass accuracy: 782.5659 and 5.023 ± 0.515). (D) Significant differences (*$p < 0.05$) in intensities between DIUTHAME-MS (m/z and intensity: 782.5663 and 65 508 470.670 ± 2 916 148.270) and MALDI-MS (m/z and intensity: 782.5659 and 10 067 074.330 ± 6 714 858.090. Values are presented as mean ± SD of three measurements. Here, *$p < 0.05$ (two-tailed t-test)

mass accuracies and intensities than MALDI-MS (Figures 5A and 5B, respectively). These results indicated that DIUTHAME-MS offers higher reproducibility in terms of mass accuracy and intensity measurements than MALDI-MS.

4 | DISCUSSION

DIUTHAME chip, a novel SALDI technique developed by our group, has shown the capability of MS analyses[46,55–57] and MSI analyses[47,48,58] of lipids in biological tissue sections. In this study, we examined the effect of DIUTHAME on the reproducibility of mass accuracies and intensities by analyzing a standard lipid as well as mouse brain tissue sections. To the best of our knowledge, this is the first study conducted through the novel combination of DIUTHAME, and FTICR MS. DIUTHAME-MS showed significantly lower fluctuations in mass errors and intensities of the measured ions than conventional MALDI-MS, where DHB was used as a matrix. These phenomena are thought to be largely attributable to the Coulombic effect reported previously.[59]

Inherently, FTICR MS offers the highest mass accuracy as well as resolving power,[60] by converting the cyclotron frequency to m/z value in a fixed magnetic field.[61,62] In modern FTICR instruments, the influence of Coulomb mutual (ion–ion and ion–image charge) interactions in ion motion is the most crucial factor in reducing high mass accuracy.[63] Each ion cloud experiences interactions with other ion clouds; this affects their specific cyclotron frequency and results in mass measurement errors. Absolute error values have been reported to be related to individual peak intensities.[28] Use of a corrected calibration function could lead to an improvement in the accuracy of the mass. However, numerical simulation is the only way of investigating the effects of ion–ion interactions.[64,65] The main factors influencing the difference in mass accuracy between MALDI and DIUTHAME could be investigated by computer simulation.

It is interesting that the mass accuracy could be altered simply by changing the means of laser desorption ionization for an FTICR instrument, especially one with an external ion source. Coulombic effects could be considered as the reason for this phenomenon. The simplest Coulombic effect is the space charge effect (mass calibration formula, Equation 1), in which an increase in the total number of ions
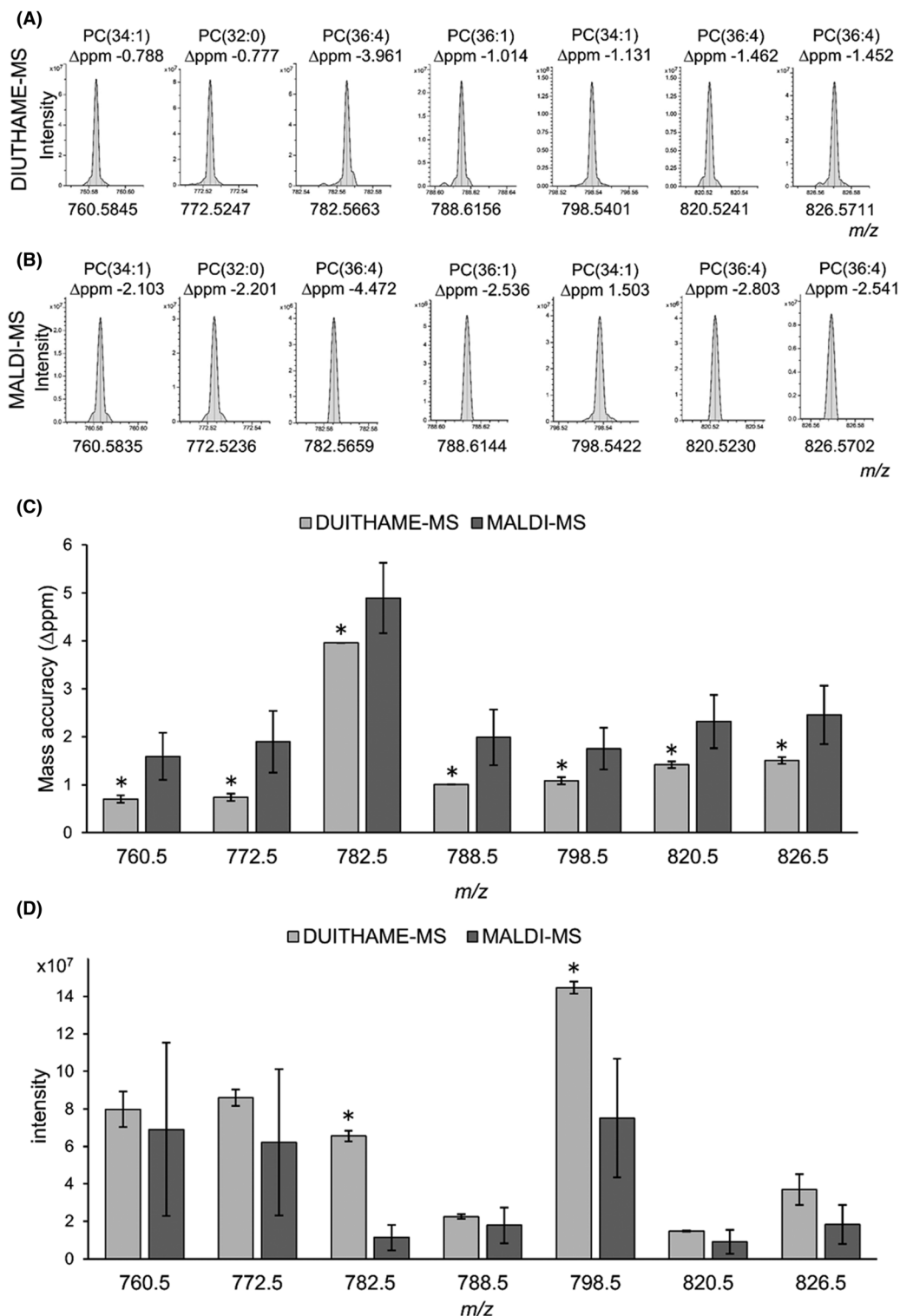
FIGURE 4 Comparison in mass accuracies and intensities of some abundant lipid ions of mouse brain tissue sections between DIUTHAME-MS and MALDI-MS. Representative ions of lipids at m/z 760.585, 772.525, 782.569, 788.616, 798.541, 720.525, and 726.573 in (A) DIUTHAME-MS and (B) MALDI-MS with their mass accuracies (expressed in Δppm). (C) Significant differences (*$p < 0.05$) in mass accuracies of all lipid ion peaks between DIUTHAME-MS (m/z and mass accuracies: 760.5845 and 0.703 ± 0.075; 772.5247 and 0.737 ± 0.075; 782.5663 and 3.961 ± 0.001; 788.6156 and 1.007 ± 0.006; 798.5401 and 1.087 ± 0.075; 820.5241 and 1.420 ± 0.069; 826.5711 and 1.490 ± 0.069) and MALDI-MS (m/z and mass accuracies: 760.5835 and 1.590 ± 0.491; 772.5236 and 1.897 ± 0.641; 782.5659 and 5.023 ± 0.515; 788.6144 and 1.987 ± 0.576; 798.5422 and 1.750 ± 0.433; 820.5230 and 2.317 ± 0.555; 826.5702 and 2.457 ± 0.609). (D) Significant differences (*$p < 0.05$) in intensities at m/z 782.56 and m/z 798.54 between DIUTHAME-MS (m/z and intensities: 782.5663 and 65 508 470.670 ± 2 916 148.270; 798.5401 and 144 645 104 ± 3 202 724.700) and MALDI-MS (m/z and intensities: 782.5659 and 10 067 074.330 ± 6 714 858.090; 798.5422 and 26 303 317 ± 31 679 462.110). DIUTHAME-MS showed a smaller SD in mass accuracy and intensity measurements for all selected ions than MALDI-MS. Values are presented as mean ± SD of three measurements. Here, *$p < 0.05$ (two-tailed t-test)
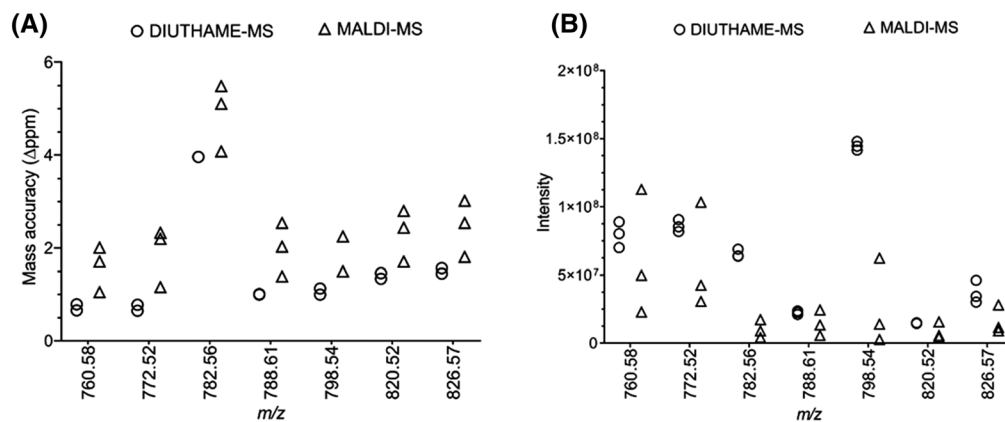
FIGURE 5 Distribution of mass accuracies and intensities for some abundant lipid ions observed in mouse brain sections in DIUTHAME-MS and MALDI-MS. Dot plot shows differences in fluctuations of mass accuracies (A) and intensities (B) of some abundant lipid ions in mouse brain sections between DIUTHAME-MS (circle) and MALDI-MS (triangle). Data acquired in three individual measurements under the same experimental conditions

trapped in the ICR cell results in a monotonic decrease in the cyclotron frequencies.[66] Regarding the result in Figure 2, where the mass spectra are dominated by the single standard lipid ions, the difference in mass accuracy can be fully explained by this space charge effect depending on the magnitude of the peak intensity. Therefore, it is predicted that the mass accuracy of MALDI-MS can be improved by intentionally reducing the number of ions trapped in the ICR cell, and the difference between MALDI and DIUTHAME is not essential. However, regarding the results in Figures 3 and 4, the relationship between mass accuracy and peak intensity is clearly reversed and cannot be explained by the simple space charge effect. Large fluctuations in the total number of ions from measurement to measurement result in a reduced mass accuracy. As expected, we observed a clear difference in the number of ion peaks between the DIUTHAME-MS and MALDI-MS spectra, where the former showed fewer contaminant ion peaks (Figures S2, supporting information). This is consistent with our previous report.[48] The trapping of low-mass matrix-derived ions in the ICR cell can be avoided if the parameters of the ion transfer system, such as the transmission m/z band of the quadrupole ion guide and the time-of-flight value for traveling to the ICR cell, are set very carefully. In this study, the ion transfer parameters were set as the conditions for detecting ions in the m/z 500–1200 range of interest with the highest sensitivity. In addition, the SD values of the measured mass accuracies are rather non-uniform over the range of mass spectra compared with the global peak shifts expected from the simplest Coulombic effect. Therefore, it is suggested that more complicated Coulombic effects, as typified by peak coalescence,[59,67-69] than the simple space charge effect have influenced the mass accuracy.

In DIUTHAME experiments, the purpose of using thick sections (30 μm) is to ensure sufficient capillary action and surface adhesion between the tissue section and the porous alumina membrane. If the thickness is less than 20 μm, the gap between the tissue section and the DIUTHAME membrane might remain after thawing. A thick section is less likely to suffer from incomplete surface adhesion than a

thinner section.[47] The DIUTHAME chip is currently being developed to minimize the gap between tissue section and membrane after mounting, ensuring proper adhesion for a section thickness of 10 μm.

DIUTHAME-MS showed higher intensity signals in the analysis of mouse brain tissue sections than MALDI-MS (Figures 3D and 4D, respectively). However, the liquid sample analysis showed the opposite results (Figure 2D). This could be due to there being insufficient sample retention on the top surface of the DIUTHAME membrane as precipitation occurs under the membrane. A high volume or concentrated liquid sample addition onto the DIUTHAME chip may overcome this problem.

5 | CONCLUSIONS

Our results demonstrated that DIUTHAME offers high reproducibility in terms of mass accuracy and intensity measurements in both liquid and mouse brain section analyses compared with MALDI-MS. It can potentially be used instead of the conventional MALDI-MS and MSI analyses to achieve highly reproducible data. Due to its high mass accuracy and intensity with high reproducibility features, DIUTHAME can be used to identify unknown compounds in non-targeted MS and MSI analyses by limiting the number of possible formulae for a given ion.

PEER REVIEW

The peer review history for this article is available at https://publons.com/publon/10.1002/rcm.9076.

ORCID

Md. Mahmudul Hasan ![ORCID icon] https://orcid.org/0000-0003-3332-1823

Md. Al Mamun ![ORCID icon] https://orcid.org/0000-0001-9274-3386

Ariful Islam ![ORCID icon] https://orcid.org/0000-0001-7497-3540

A.S.M. Waliullah ![ORCID icon] https://orcid.org/0000-0001-6778-379X

Do Huu Chi ![ORCID icon] https://orcid.org/0000-0001-9231-6843

Yasuhide Naito ![ORCID icon] https://orcid.org/0000-0002-1880-7377

Mitsutoshi Setou ![ORCID icon] https://orcid.org/0000-0002-1302-6467

REFERENCES

1. Eriksson C, Masaki N, Yao I, Hayasaka T, Setou M. MALDI imaging mass spectrometry: A mini review of methods and recent developments. *Mass Spectrom*. 2013;2(Special_Issue):S0022. https://doi.org/10.5702/massspectrometry.s0022

2. Wiseman JM, Ifa DR, Song Q, Cooks RG. Tissue imaging at atmospheric pressure using desorption electrospray ionization (DESI) mass spectrometry. *Angew Chem Int Ed*. 2006;45(43):7188-7192. https://doi.org/10.1002/anie.200602449

3. Anderton CR, Gamble LJ. Secondary ion mass spectrometry imaging of tissues, cells, and microbial systems. *Micros Today*. 2016;24(2):24-31. https://doi.org/10.1017/s1551929516000018

4. Caprioli RM, Farmer TB, Gile J. Molecular imaging of biological samples: Localization of peptides and proteins using MALDI-TOF MS. *Anal Chem*. 1997;69(23):4751-4760. https://doi.org/10.1021/ac970888i

5. Al Mamun M, Sato S, Naru E, et al. Higher accumulation of docosahexaenoic acid in the vermilion of the human lip than in the skin. *Int J Mol Sci*. 2020;21(8):2807. https://doi.org/10.3390/ijms21082807

6. Zemski Berry KA, Hankin JA, Barkley RM, Spraggins JM, Caprioli RM, Murphy RC. MALDI imaging of lipid biochemistry in tissues by mass spectrometry. *Chem Rev*. 2011;111(10):6491-6512. https://doi.org/10.1021/cr200280p

7. Islam A, Takeyama E, Mamun MA, et al. Green nut oil or DHA supplementation restored decreased distribution levels of DHA containing phosphatidylcholines in the brain of a mouse model of dementia. *Metabolites*. 2020;10(4):153. https://doi.org/10.3390/metabo10040153

8. Nakashima Y, Setou M. Distribution of antisense oligonucleotides in rat eyeballs using MALDI imaging mass spectrometry. *Mass Spectrom*. 2018;7(1):A0070. https://doi.org/10.5702/massspectrometry.a0070

9. Eto F, Sato S, Setou M, Yao I. Region-specific effects of scrapper on the abundance of glutamate and gamma-aminobutyric acid in the mouse brain. *Sci Rep*. 2020;10(1):1-10. https://doi.org/10.1038/s41598-020-64277-w

10. Cornett DS, Frappier SL, Caprioli RM. MALDI-FTICR imaging mass spectrometry of drugs and metabolites in tissue. *Anal Chem*. 2008;80(14):5648-5653. https://doi.org/10.1021/ac800617s

11. Sugiura Y, Setou M. Imaging mass spectrometry for visualization of drug and endogenous metabolite distribution: Toward in situ pharmacometabolomes. *J Neuroimmune Pharmacol*. 2010;5(1):31-43. https://doi.org/10.1007/s11481-009-9162-6

12. Sugiura Y, Setou M, Horigome D. Matrix choice. In: *Imaging Mass Spectrometry*. Japan: Springer; 2010:55-69. https://doi.org/10.1007/978-4-431-09425-8_5.

13. Nakashima Y, Eto F, Ishihara K, et al. Development of sheet-enhanced technique (SET) method for matrix-assisted laser desorption/ionization imaging mass spectrometry. *Rapid Commun Mass Spectrom*. 2020;34(8):e8703. https://doi.org/10.1002/rcm.8703

14. Williams TL, Andrzejewski D, Lay JO, Musser SM. Experimental factors affecting the quality and reproducibility of MALDI TOF mass spectra obtained from whole bacteria cells. *J Am Soc Mass Spectrom*. 2003;14(4):342-351. https://doi.org/10.1016/S1044-0305(03)00065-5

15. Lai Y-H, Wang Y-S. Matrix-assisted laser desorption/ionization mass spectrometry: Mechanistic studies and methods for improving the structural identification of carbohydrates. *Mass Spectrom*. 2017;6(3):S0072. https://doi.org/10.5702/massspectrometry.S0072

16. O'Rourke MB, Raymond BBA, Padula MP. The characterization of laser ablation patterns and a new definition of resolution in matrix assisted laser desorption ionization imaging mass spectrometry (MALDI-IMS). *J Am Soc Mass Spectrom*. 2017;28(5):895-900. https://doi.org/10.1007/s13361-017-1632-0

17. Li YL, Gross ML, Hsu FF. Ionic-liquid matrices for improved analysis of phospholipids by MALDI-TOF mass spectrometry. *J Am Soc Mass Spectrom*. 2005;16(5):679-682. https://doi.org/10.1016/j.jasms.2005.01.017

18. Abdelhamid HN. Ionic liquid-assisted laser desorption/ionization–mass spectrometry: Matrices, microextraction, and separation. *Methods Protoc*. 2018;1(2):23. https://doi.org/10.3390/mps1020023

19. Lim L, Yan F, Bach S, Pihakari K, Klein D. Fourier transform mass spectrometry: The transformation of modern environmental analyses. *Int J Mol Sci*. 2016;17(1):104. https://doi.org/10.3390/ijms17010104

20. Amster IJ. Fourier transform mass spectrometry. *J Mass Spectrom*. 1996;31(12):1325-1337. https://doi.org/10.1002/(SICI)1096-9888(199612)31:12%3C1325::AID-JMS453%3E3.0.CO;2-W

21. Kind T, Fiehn O. Metabolomic database annotations via query of elemental compositions: Mass accuracy is insufficient even at less than 1 ppm. *BMC Bioinformatics*. 2006;7(1):234. https://doi.org/10.1186/1471-2105-7-234

22. Marshall AG. Milestones in Fourier transform ion cyclotron resonance mass spectrometry technique development. *Int J Mass Spectrom*. 2000;200(1-3):331-356. https://doi.org/10.1016/S1387-3806(00)00324-9

23. Easterling ML, Mize TH, Amster IJ. Routine part-per-million mass accuracy for high-mass ions: Space-charge effects in MALDI FT-ICR. *Anal Chem*. 1999;71(3):624-632. https://doi.org/10.1021/ac980690d

24. Burton RD, Matuszak KP, Watson CH, Eyler JR. Exact mass measurements using a 7 tesla Fourier transform ion cyclotron resonance mass spectrometer in a good laboratory practices-regulated environment. *J Am Soc Mass Spectrom*. 1999;10(12):1291-1297. https://doi.org/10.1016/S1044-0305(99)00106-3

25. Bowman AP, Blakney GT, Hendrickson CL, Ellis SR, Heeren RMA, Smith DF. Ultra-high mass resolving power, mass accuracy, and dynamic range MALDI mass spectrometry imaging by 21-T FT-ICR MS. *Anal Chem*. 2020;92(4):3133-3142. https://doi.org/10.1021/acs.analchem.9b04768

26. Scigelova M, Hornshaw M, Giannakopulos A, Makarov A. Fourier transform mass spectrometry. *Mol Cell Proteomics*. 2011;10(7):M111.009431. https://doi.org/10.1074/mcp.M111.009431

27. Al Mamun M, Gonzalez TV, Islam A, et al. Analysis of potential anti-aging beverage Pru, a traditional Cuban refreshment, by desorption electrospray ionization-mass spectrometry and FTICR tandem mass spectrometry. *J Food Drug Anal*. 2019;27(4):833-840. https://doi.org/10.1016/j.jfda.2019.05.004

28. Masselon C, Tolmachev AV, Anderson GA, Harkewicz R, Smith RD. Mass measurement errors caused by "local" frequency perturbations in FTICR mass spectrometry. *J Am Soc Mass Spectrom*. 2002;13(1):99-106. https://doi.org/10.1016/S1044-0305(01)00333-6

29. Shi CY, Deng CH. Recent advances in inorganic materials for LDI-MS analysis of small molecules. *Analyst*. 2016;141(10):2816-2826. https://doi.org/10.1039/c6an00220j

30. Lu M, Yang X, Yang Y, Qin P, Wu X, Cai Z. Nanomaterials as assisted matrix of laser desorption/ionization time-of-flight mass spectrometry for the analysis of small molecules. *Nanomaterials*. 2017;7(4). https://doi.org/10.3390/nano7040087

31. Chu H-W, Unnikrishnan B, Anand A, Mao J-Y, Huang C-C. Nanoparticle-based laser desorption/ionization mass spectrometric

analysis of drugs and metabolites. *J Food Drug Anal*. 2018; 261215-1228(4):1215-1228. https://doi.org/10.1016/j.jfda.2018. 07.001

32. Vidová V, Novák P, Strohalm M, Pól J, Havlíček V, Volný M. Laser desorption-ionization of lipid transfers: Tissue mass spectrometry imaging without MALDI matrix. *Anal Chem*. 2010;82(12):4994-4997. https://doi.org/10.1021/ac100661h

33. Thomas JJ, Shen Z, Crowell JE, Finn MG, Siuzdak G. Desorption/ionization on silicon (DIOS): A diverse mass spectrometry platform for protein characterization. *Proc Natl Acad Sci*. 2001;98(9): 4932-4937. https://doi.org/10.1073/pnas.081069298

34. Liu Q, Guo Z, He L. Mass spectrometry imaging of small molecules using desorption/ionization on silicon. *Anal Chem*. 2007;79(10): 3535-3541. https://doi.org/10.1021/ac0611465

35. Go EP, Apon JV, Luo G, et al. Desorption/ionization on silicon nanowires. *Anal Chem*. 2005;77(6):1641-1646. https://doi.org/10. 1021/ac048460o

36. Northen TR, Yanes O, Northen MT, et al. Clathrate nanostructures for mass spectrometry. *Nature*. 2007;449(7165):1033-1036. https:// doi.org/10.1038/nature06195

37. Wen X, Dagan S, Wysocki VH. Small-molecule analysis with silicon-nanoparticle-assisted laser desorption/ionization mass spectrometry. *Anal Chem*. 2007;79(2):434-444. https://doi.org/10.1021/ac061154l

38. Walker BN, Stolee JA, Pickel DL, Retterer ST, Vertes A. Tailored silicon nanopost arrays for resonant nanophotonic ion production. *J Phys Chem C*. 2010;114(11):4835-4840. https://doi.org/10.1021/ jp9110103

39. Walker BN, Stolee JA, Vertes A. Nanophotonic ionization for ultratrace and single-cell analysis by mass spectrometry. *Anal Chem*. 2012;84(18):7756-7762. https://doi.org/10.1021/ac301238k

40. Morris NJ, Anderson H, Thibeault B, Vertes A, Powell MJ, Razunguzwa TT. Laser desorption ionization (LDI) silicon nanopost array chips fabricated using deep UV projection lithography and deep reactive ion etching. *RSC Adv*. 2015;5(88):72051-72057. https://doi. org/10.1039/c5ra11875a

41. Korte AR, Stopka SA, Morris N, Razunguzwa T, Vertes A. Large-scale metabolite analysis of standards and human serum by laser desorption ionization mass spectrometry from silicon nanopost arrays. *Anal Chem*. 2016;88(18):8989-8996. https://doi.org/10.1021/ acs.analchem.6b01186

42. Stopka SA, Rong C, Korte AR, et al. Molecular imaging of biological samples on nanophotonic laser desorption ionization platforms. *Angew Chem Int Ed*. 2016;55(14):4482-4486. https://doi.org/10. 1002/anie.201511691

43. Stopka SA, Holmes XA, Korte AR, Compton LR, Retterer ST, Vertes A. Trace analysis and reaction monitoring by nanophotonic ionization mass spectrometry from elevated bowtie and silicon nanopost arrays. *Adv Funct Mater*. 2018;28(29):1801730. https://doi.org/10.1002/ adfm.201801730

44. Korte AR, Morris NJ, Vertes A. High throughput complementary analysis and quantitation of metabolites by MALDI- and silicon nanopost array-laser desorption/ionization-mass spectrometry. *Anal Chem*. 2019;91(6):3951-3958. https://doi.org/10.1021/acs. analchem.8b05074

45. Muthu M, Gopal J, Chun S. Nanopost array laser desorption ionization mass spectrometry (NAPA-LDI MS): Gathering moss? *TrAC Trends Anal Chem*. 2017;97:96-103. https://doi.org/10.1016/j.trac. 2017.08.016

46. Naito Y, Kotani M, Ohmura T. A novel laser desorption/ionization method using through hole porous alumina membranes. *Rapid Commun Mass Spectrom*. 2018;32(21):1851-1858. https://doi.org/10. 1002/rcm.8252

47. Kuwata K, Itou K, Kotani M, Ohmura T, Naito Y. DIUTHAME enables matrix-free mass spectrometry imaging of frozen tissue sections. *Rapid Commun Mass Spectrom*. 2020;34(9):e8729. https://doi.org/10. 1002/rcm.8729

48. Naito Y, Kotani M, Ohmura T. Feasibility of acetylcholinesterase reaction assay monitoring in DIUTHAME-MS. *J Am Soc Mass Spectrom*. 2020;31(10):2154-2160. https://doi.org/10.1021/jasms. 0c00255

49. Ledford EB, Rempel DL, Gross ML. Space charge effects in Fourier transform mass spectrometry. Mass calibration. *Anal Chem*. 1984; 56(14):2744-2748. https://doi.org/10.1021/ac00278a027

50. Mohammadi AS, Phan NTN, Fletcher JS, Ewing AG. Intact lipid imaging of mouse brain samples: MALDI, nanoparticle-laser desorption ionization, and 40 keV argon cluster secondary ion mass spectrometry. *Anal Bioanal Chem*. 2016;408(24):6857-6868. https:// doi.org/10.1007/s00216-016-9812-5

51. Fincher JA, Dyer JE, Korte AR, Yadavilli S, Morris NJ, Vertes A. Matrix-free mass spectrometry imaging of mouse brain tissue sections on silicon nanopost arrays. *J Comp Neurol*. 2019;527(13): 2101-2121. https://doi.org/10.1002/cne.24566

52. Tempez A, Ugarov M, Egan T, et al. Matrix implanted laser desorption ionization (MILDI) combined with ion mobility-mass spectrometry for bio-surface analysis. *J Proteome Res*. 2005;4(2):540-545. https://doi. org/10.1021/pr0497879

53. Angerer TB, Dowlatshahi M, Fletcher JS. Improved molecular imaging in rodent brain with time-of-flight-secondary ion mass spectrometry using gas cluster ion beams and reactive vapor exposure. *Anal Chem*. 2015;87(8):4305-4313. https://doi.org/10.1021/ac504774y

54. Passarelli MK, Winograd N. Lipid imaging with time-of-flight secondary ion mass spectrometry (ToF-SIMS). *Biochim Biophys Acta Mol Cell Biol Lipids*. 2011;1811(11):976-990. https://doi.org/10. 1016/j.bbalip.2011.05.007

55. Sato H, Nakamura S, Fouquet T, Ohmura T, Kotani M, Naito Y. Molecular characterization of polyethylene oxide based oligomers by surface-assisted laser desorption/ionization mass spectrometry using a through-hole alumina membrane as active substrate. *Rapid Commun Mass Spectrom*. 2020;34(5):e8597. https://doi.org/10.1002/ rcm.8597

56. Sato H, Nakamura S, Fouquet TNJ, Ohmura T, Kotani M, Naito Y. Simple pretreatment for the analysis of additives and polymers by surface-assisted laser desorption/ionization mass spectrometry using a through-hole alumina membrane as a functional substrate. *J Am Soc Mass Spectrom*. 2020;31(2):298-307. https://doi.org/10.1021/jasms. 9b00048

57. Fouquet TNJ, Cody RB, Nakamura S, et al. Rapid fingerprinting of high-molecular-weight polymers by laser desorption-ionization using through-hole alumina membrane high-resolution mass spectrometry. *Anal Chem*. 2020;92(11):7399-7403. https://doi.org/10.1021/acs. analchem.0c01070

58. Enomoto H, Kotani M, Ohmura T. Novel blotting method for mass spectrometry imaging of metabolites in strawberry fruit by desorption/ionization using through hole alumina membrane. *Foods*. 2020;9(4):408. https://doi.org/10.3390/foods9040408

59. Mitchell DW, Smith RD. Cyclotron motion of two Coulombically interacting ion clouds with implications to Fourier-transform ion cyclotron resonance mass spectrometry. *Phys Rev E*. 1995;52(4): 4366-4386. https://doi.org/10.1103/PhysRevE.52.4366

60. Erve JCL, DeMaio W, Talaat RE. Rapid metabolite identification with sub parts-per-million mass accuracy from biological matrices by direct infusion nanoelectrospray ionization after clean-up on a ZipTip and LTQ/Orbitrap mass spectrometry. *Rapid Commun Mass Spectrom*. 2008;22(19):3015-3026. https://doi.org/10.1002/rcm.3702

61. Comisarow MB, Marshall AG. The early development of Fourier transform ion cyclotron resonance (FT-ICR) spectroscopy. *J Mass Spectrom*. 1996;31(6):581-585. https://doi.org/10.1002/(SICI)1096-9888(199606)31:6%3C581::AID-JMS369%3E3.0.CO;2-1

62. Marshall AG, Hendrickson CL, Jackson GS. Fourier transform ion cyclotron resonance mass spectrometry: A primer. *Mass Spectrom Rev*. 1998;17(1):1-35. https://doi.org/10.1002/(SICI)1098-2787(1998)17:1%3C1::AID-MAS1%3E3.0.CO;2-K

63. Nikolaev EN, Kostyukevich YI, Vladimirov GN. Fourier transform ion cyclotron resonance (FT ICR) mass spectrometry: Theory and simulations. *Mass Spectrom Rev*. 2016;35(2):219-258. https://doi.org/10.1002/mas.21422

64. Leach FE, Kharchenko A, Heeren RMA, Nikolaev E, Amster IJ. Comparison of particle-in-cell simulations with experimentally observed frequency shifts between ions of the same mass-to-charge in Fourier transform ion cyclotron resonance mass spectrometry. *J Am Soc Mass Spectrom*. 2010;21(2):203-208. https://doi.org/10.1016/j.jasms.2009.10.001

65. Aizikov K, O'Connor PB. Use of the filter diagonalization method in the study of space charge related frequency modulation in Fourier transform ion cyclotron resonance mass spectrometry. *J Am Soc Mass Spectrom*. 2006;17(6):836-843. https://doi.org/10.1016/j.jasms.2006.02.018

66. Jeffries JB, Barlow SE, Dunn GH. Theory of space-charge shift of ion cyclotron resonance frequencies. *Int J Mass Spectrom Ion Process*. 1983;54(1-2):169-187. https://doi.org/10.1016/0168-1176(83)85016-2

67. Hendrickson CL, Beu SC, Laude DA. Two-dimensional coulomb-induced frequency modulation in Fourier transform ion cyclotron resonance: A mechanism for line broadening at high mass and for large ion populations. *J Am Soc Mass Spectrom*. 1993;4(12):909-916. https://doi.org/10.1016/1044-0305(93)80016-R

68. Naito Y, Inoue M. Peak confluence phenomenon in Fourier transform ion cyclotron resonance mass spectrometry. *J Mass Spectrom Soc Jpn*. 1994;42(1):1-9. https://doi.org/10.5702/massspec.42.1

69. Naito Y, Inoue M. Collective motion of ions in an ion trap for Fourier transform ion cyclotron resonance mass spectrometry. *Int J Mass Spectrom Ion Process*. 1996;157-158:85-96. https://doi.org/10.1016/S0168-1176(96)04467-9

SUPPORTING INFORMATION

Additional supporting information may be found online in the Supporting Information section at the end of this article.